

Modelling of Welding Processes – Applied Models and Examples

Abstract: The article aims to present the manner in which welding processes are modelled using dedicated software programmes, provides examples concerning applications of various heat sources and indicates the necessity of performing tests aimed to increase the consistence of simulation results with those obtained in experimental verification.

Keywords: FEM, heat source, heat input, heat flow, liquid metal pool

DOI: [10.17729/ebis.2017.6/4](https://doi.org/10.17729/ebis.2017.6/4)

Introduction

At present, the simulation of welding processes is based on two models of welding heat sources, i.e. the Goldak and the Gaussian model. These models are used to forecast changes in the liquid metal pool and in the material subjected to welding (by simulating the above-named phenomena using the Finite Element Method (FEM)). The models enable the relatively accurate simulation of welding processes and make it possible to forecast the effect of related factors on the behaviour of the liquid metal pool and that of the base material. The modelling of welding processes enables the minimisation or even the elimination of undesired results of welding processes such as welding stresses and strains or unfavourable structures. Consequently, the use of modelling makes it possible to reduce costs incurred in industry primarily before starting the fabrication of new elements or welded units.

Welding processes involve physical phenomena of metallurgic and thermodynamic nature.

For this reason, the modelling of welding processes requires a number of simplifications (based on empirical tests) increasing the certainty of modelled processes and that of the behaviour of welded materials in relation to factors affecting both the liquid metal pool and the material subjected to welding.

To present the selection of an appropriate model when simulating welding processes, it is necessary to take a closer look at the effect of various factors taking place in welding (i.e. a special process) [1] on the geometrical shape of the liquid metal pool.

Applied Models of Welding Processes

The combination of all of the factors affecting the flow of heat between the heat source and the element subjected to welding as well as in the material itself triggers the formation of the liquid metal pool. In spite of that heat distribution and the weld pool shape are strictly correlated, when simulating welding processes these factors are not taken into consideration

separately as they are numerous and affect one another. This could significantly impede the simulation process because of an enormous increase in time and in the number of calculations. As a result, adopted heat models are those the form of which is identified analytically. The geometrical heat source model is modified by taking into consideration a welding method, process thermodynamics, material properties and welding process parameters [2, 3]. Apart from the two commonly used models of welding heat sources, i.e. the Goldak model and the Gaussian model [4], it is also possible to use models combining the Goldak model and the Gaussian model [5]. Because of its geometrical form, the Goldak model (presented in Figure 1) is also referred to as the double ellipsoid model. This model is frequently used when modelling arc welding processes using the MIG, MAG, TIG and SAW, i.e. low and medium-energy processes. The dimensions of the double ellipsoid are determined by parameters C_r , C_f , a and b in Figure 1, corresponding to geometrical dimensions of a liquid metal pool. The Goldak model allows for the presence of zones having various temperature and, consequently, varying amounts of heat emitted in the front and back half of the ellipsoid [2, 3, 6, 7].

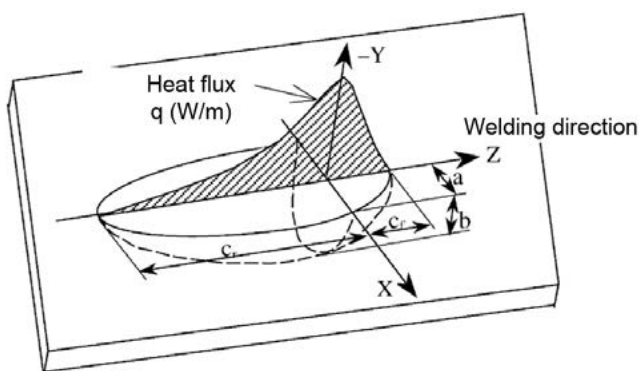


Fig. 1. Goldak heat source model [8]

The information about the use of the Goldak model in the modelling of heat sources can be found in relation to numerous tests, the results of which were provided in various scientific studies [9, 10]. Selected test results are presented in the remainder of this publication.

TIG Welding

The distribution of heat and the shape of the liquid metal pool during TIG welding are presented in Figure 2. The results were obtained when melting a disc (having a diameter of 10.8 cm) made of steel AISI 1005. The welds were made using the TIG method, a constant power of 1.9 kW (110 A, 1.5 V), a tungsten electrode (having a diameter of 4.7 mm) containing a 2% thorium addition. High purity helium (99.999%), I2 according to PN-EN ISO 14175, was used as shielding and welding gas (99.999%). The steel disc rotated at a constant rate of 0.11 rpm in relation to the tungsten electrode (which corresponds a rate of 0.6 mm/s) [11].

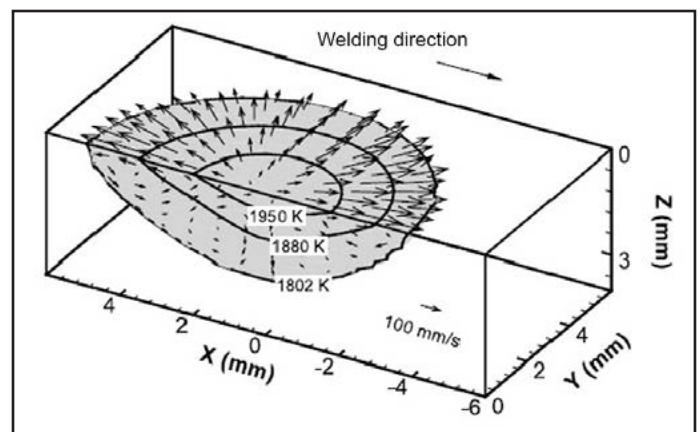


Fig. 2. Three-dimensional schematic diagram presenting temperature distribution and areas of the liquid metal pool in the TIG method [11]

Figures 2 and 3 present the geometrical shape of the liquid metal pool developed on the basis of X-ray tests and metallographic specimens. The fusion line and HAZ boundaries are presented using dashed lines in Figure 3. The isotherms were indicated on the basis of the 3D model of the flow of heat and that of fluid. The liquidus isotherm (1802 K) determined on the basis of the model coincided with measurements performed on the liquid weld pool. The same applies to eutectoid temperature [11].

The Goldak model simulates temperature differences in front of and behind the weld pool, yet the model adopts the shape of ellipsis, not always corresponding to the geometrical shape of the liquid metal pool in Figure 4.

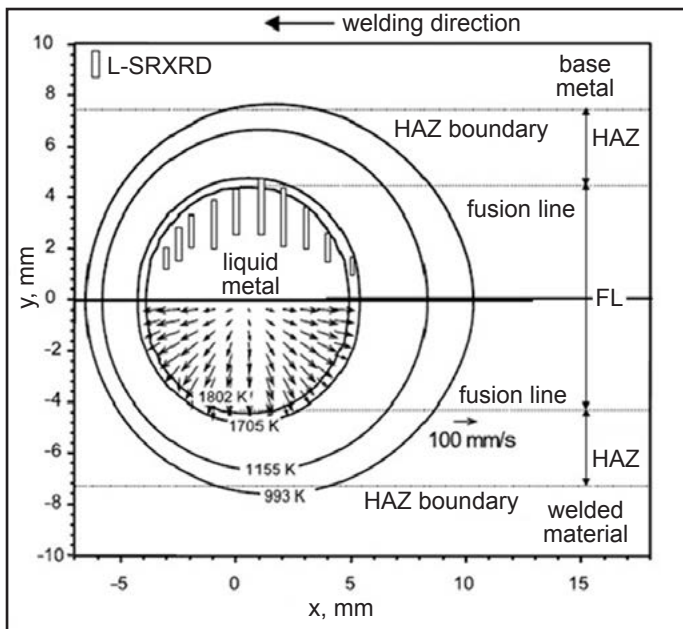


Fig. 3. Two-dimensional model presenting temperature distribution and liquid metal pool areas in the TIG method [11]

The presented geometrical shape of the weld pool depended on a heat input and welding rate V . The weld pool became elongated changing its shape from elliptical into that of a falling drop [12].

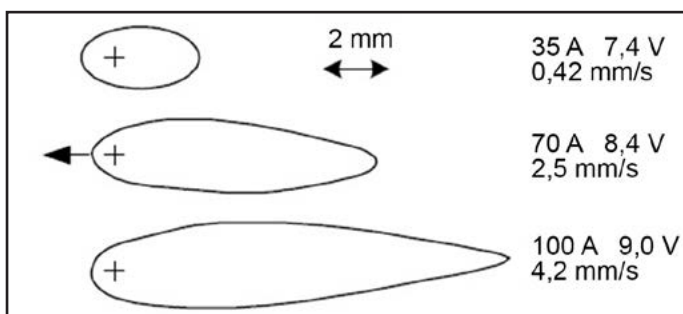


Fig. 4. Shape of the liquid metal pool during the TIG welding of stainless steel 304 [12]

The model of heat source having the form of the Gaussian curve is used in simulations of welding processes involving the use of high-energy welding methods (electron beam welding, laser welding, plasma welding etc.). The Gaussian model represents geometrical shapes of welds, i.e. deep penetration and a slight penetration width, characteristic of key-hole welding. The precise geometrical form of heat distribution depends on a welding method and its parameters as well as on the thickness, temperature and physical properties of the material subjected to welding [2, 13, 14, 15]. The Gaussian model is presented in Figure 5.

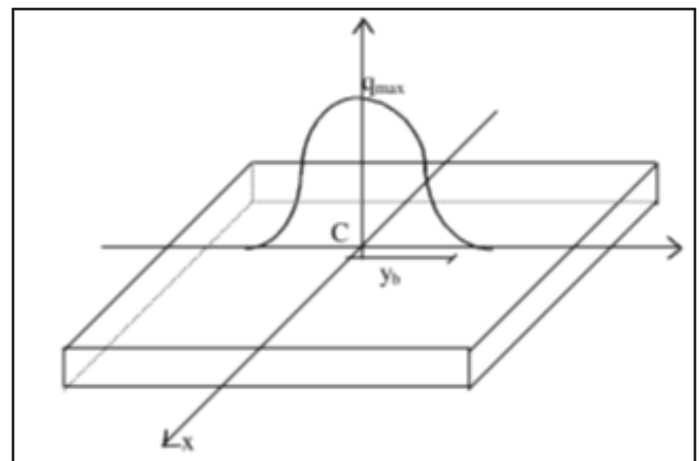


Fig. 5. Heat distribution on the material surface in the Gaussian curve form [15]

Discussed below is the practical application of the Gaussian model-based simulation of welding processes.

Plasma Welding

The geometrical shape of the liquid metal pool during plasma welding with full penetration was identified through tests involving sheets made of austenitic stainless steel and parameters presented in Table 1 for two cases, i.e. (A) and (B) varying in welding current [16].

Table 1. Plasma welding parameters [16]

| Parameter | Value, unit |
|---|-------------|
| Torch diameter | 3.8 mm |
| Distance between the torch and the element subjected to welding | 6 mm |
| Shielding gas flow rate (Ar 99.99%) | 20 l/min |
| Plasma gas flow rate (Ar 99.99%) | 3 l/min |
| Arc voltage | 24.2 V |
| Arc current (A) | 169.0 A |
| Arc current (B) | 180.0 A |

Figure 6 depicts the weld pool progressing into the base material as well as the flow of liquid metal in plasma welding. After arc striking, the base material was heated by plasma arc and formed a small liquid metal pool – 0.27 s (a). The formation of the weld pool was followed by its gradual growth (b-e). When observing schematic diagrams c through h it is possible to notice a significant increase in the depth of penetration in the base material, yet not exceeding the thickness of a sheet subjected to welding. The

Laser Welding

flow-through channel changed from U-shaped into V-shaped (c-f). The complete melting of the element subjected to welding occurred after 1.72 s. Afterwards, the significant widening of the channel took place (k-n) [16]. In case (B) for a current of 180 A, full penetration occurred faster by 0.16 s [16].

The geometrical shape of the liquid metal pool during laser welding with full penetration is similar to that obtained during plasma welding. Tests imaging the geometrical shape of the liquid metal pool were performed using lenses GaAs having a focal power of 100 mm, a laser beam power of 600 W and a laser beam diameter

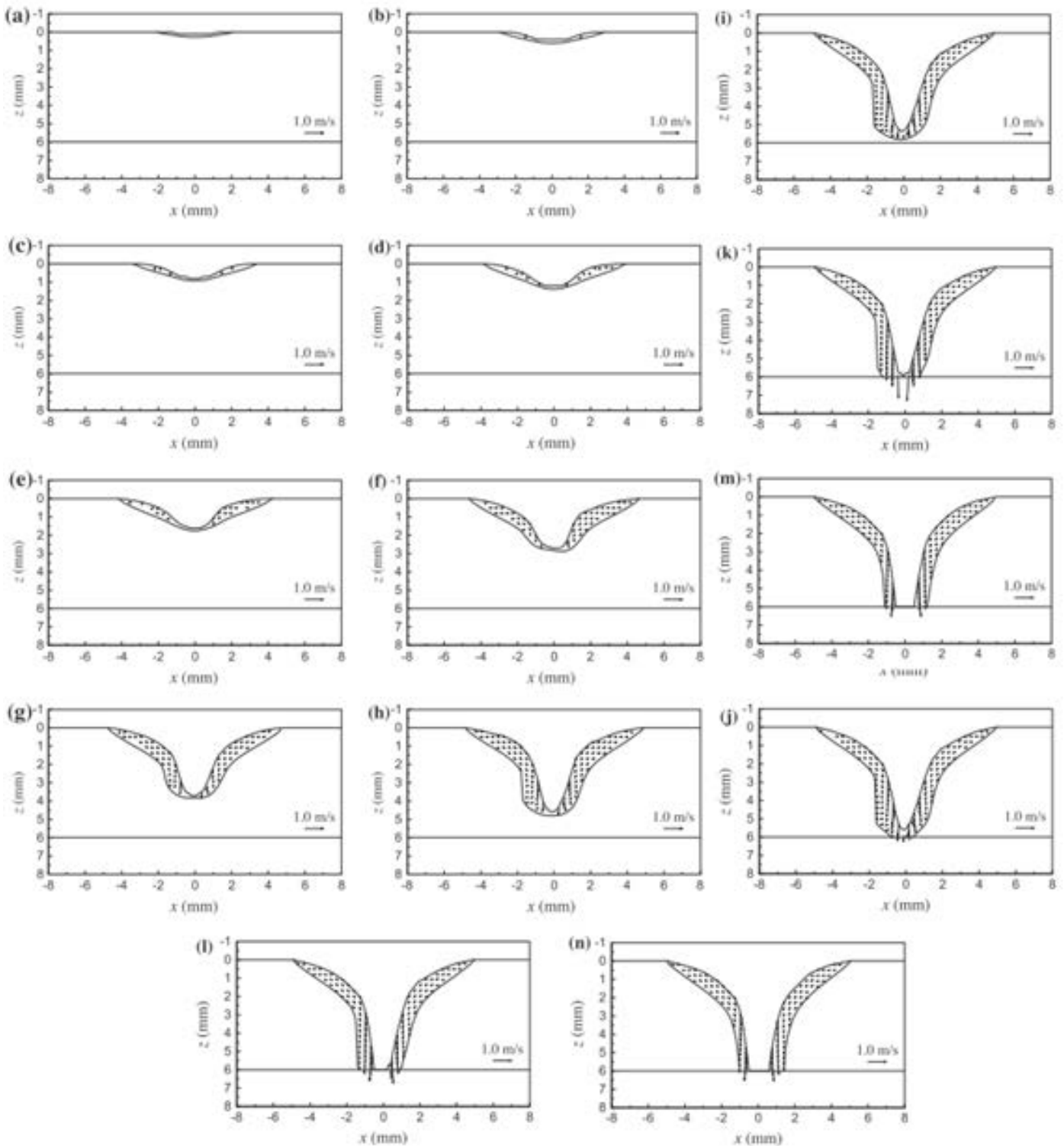


Fig. 6. Progressive increase in the weld pool, flow-through channel and the liquid metal flow rate, case (A): (a) $t = 0.27$ s; (b) $t = 0.38$ s; (c) $t = 0.50$ s; (d) $t = 0.71$ s; (e) $t = 0.91$ s; (f) $t = 1.34$ s, (g) $t = 1.50$ s; (h) $t = 1.62$ s; (i) $t = 1.71$ s; (j) $t = 1.72$ s; (k) $t = 1.73$ s; (l) $t = 1.74$ s; (m) $t = 1.80$ s; (n) $t = 1.86$ s [16]

(before focusing) of 15 mm as well as using a welding rate of 10 mm/s. The lenses were cooled using compressed air. The shielding gas used in the process was argon (99.999%Ar). The experiment involved the use of glass GG17 characterised by high heat resistance and a significant difference between the melting point and the evaporation point. Figure 7 presents a typical cross-section of the liquid metal pool in laser welding. To develop heat distribution around the liquid metal pool, it was divided into layers (Fig. 8) [17].

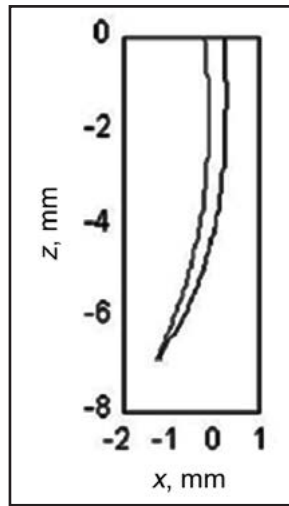


Fig. 7. Model of a typical liquid metal pool during laser welding with full penetration [17]

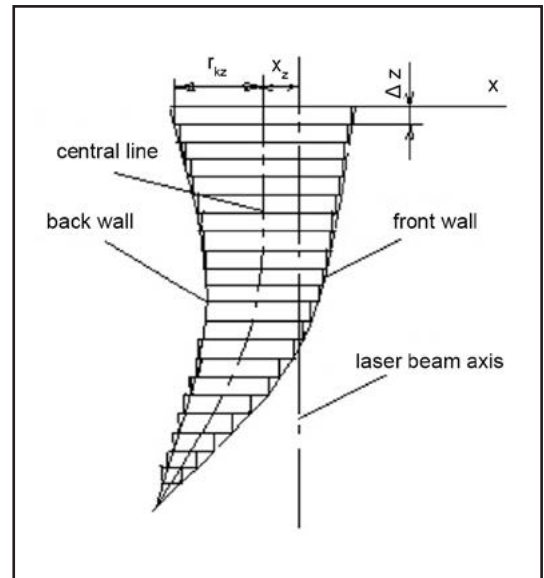


Fig. 8. Schematic diagram presenting the liquid metal pool divided into layers [17]

The following assumptions were adopted when creating the heat conductivity model [17]:

- conductivity along the z-axis was ignored (Fig. 7); as a result, the heat conductivity model was reduced to two dimensions,
- in relation to each segment on the z-axis, the liquid metal pool was treated as a cylinder (with a changing diameter and position in relation to the z-axis),
- temperature on each wall was assumed to be the metal evaporation point, yet the evaporation energy of a small material particle was ignored,
- convection heat was ignored,
- process was recognised as stable,
- glass properties were dependent on temperature; the values of properties were adopted at a temperature of 870 K.

A related thermal conductivity model (see Fig. 9) was developed following the adopted assumptions. Based on the model it was ascertained that the highest temperature was around the liquid metal pool (thermal conductivity of GG15 is very low).

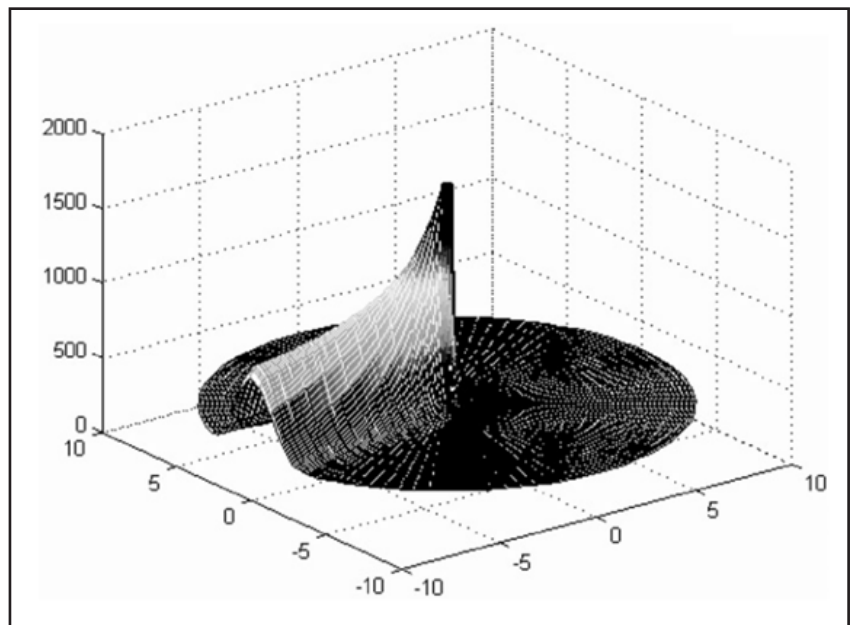


Fig. 9. Temperature distribution on the surface of the material subjected to welding [17]

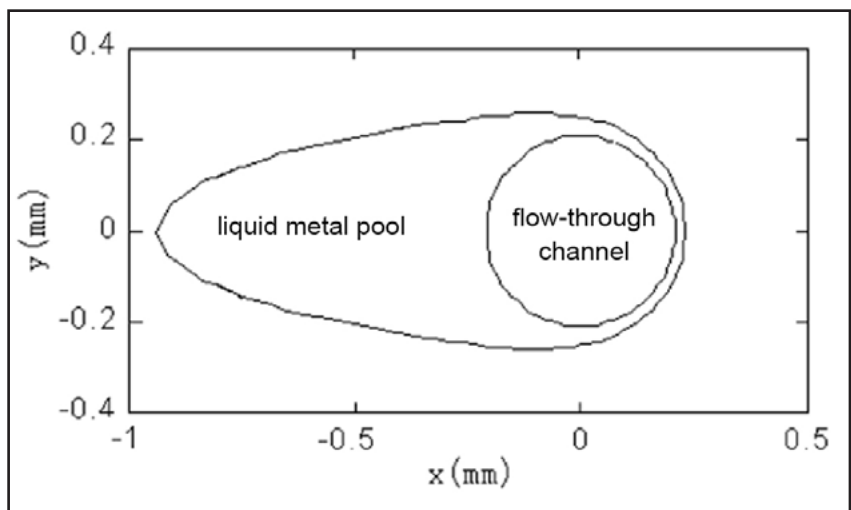


Fig. 10. Shape of the liquid metal pool on the surface of the material being welded [17] /liquid metal pool; flow-through channel

Figure 10 presents the shape of the weld pool on the surface of the material subjected to welding; the shape refers to each of the layers presented in Figure 9. The liquid metal pool grew in the direction opposite to that of welding [17].

Based on the above-presented model it was possible to present the approximate shape of the liquid metal pool on the surface of the material being welded in relation to various welding rates (see Fig. 11). The diameter of the flow-through channel amounted to 0.32 mm, whereas the numbers in the schematic diagram represent welding rate values expressed in mm/min [17].

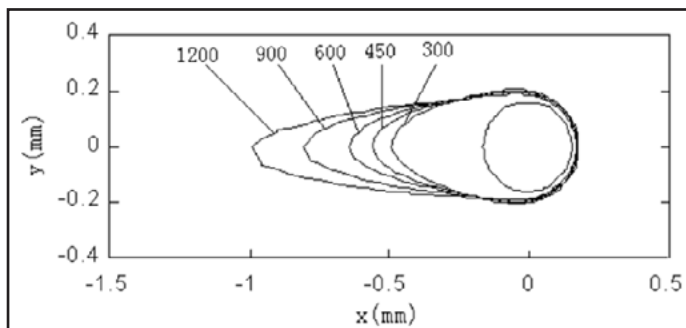


Fig. 11. Shape of the liquid metal pool on the surface of the material being welded in relation to various welding rates [17]

Figure 12 presents the shape of the liquid metal pool in relation to the diameter of the flow-through channel. The welding rate amounted to 600 mm/min; the numbers in the schematic diagram represent diameter of the flow-through channel in mm. An increase in the flow-through channel diameter was accompanied by an increase in the length and that in the width of the liquid metal pool [17].

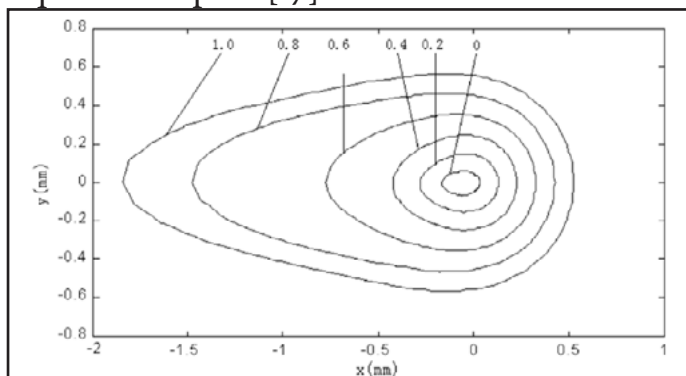


Fig. 12. Shape of the liquid metal pool on the surface of the material being welded in relation to the flow-through channel diameter [17]

As can be seen in examples prepared in the article, two, i.e. Goldak and Gauss, models are used when modelling heat sources used in welding processes. The first model relatively well corresponds to the geometrical shape of the liquid metal pool where arc welding power sources (e.g. MIG, MAG or SAW), i.e. used in low and medium-energy processes, are modelled. The Gauss model, used when modelling high-energy welding power sources (e.g. plasma, laser or EBW) properly models penetration depth and width accompanying the above-named processes. However, it is necessary to additionally consider changes occurring in the geometrical shape of the liquid metal pool. In such cases, particularly useful are combined modelling methods based on the Gauss model, used for the modelling of the liquid metal pool depth and width, and the Goldak model, enabling the modelling of the liquid metal pool shape on the surface of a material subjected to welding.

Summary

In order for computer simulations of welding processes to better model actual changes in the shape of the liquid metal pool and its effect on the material subjected to welding it is necessary to perform tests involving various materials and welding parameters. By doing so, software programmes assisting welding processes (e.g. ANSYS and SYSWELD) will better forecast joint behaviour and changes in joint properties. An example of a successfully performed computer simulation of a welding process could be a test involving steel X2CrNiMoN22-5-3 performed in 2016 [18].

References

- [1] PN-EN ISO 9001:2001. *Quality management systems – Requirements*
- [2] “How to model a welding heat source”, ESI Group presentation
- [3] Hongyuan F., Qingguo M., Wenli Xu, Shude Ji: *New General Double Ellipsoid Heat Source Model*. Science and

- Technology of Welding and Joining, 2005, vol. 10, no. 3, pp. 361-368.
<http://dx.doi.org/10.1179/174329305x40705>
- [4] Rogalski D., Golański D., Chmielewski T.: *Modele spawalniczych źródeł ciepła w analizie pola temperatury*. Przegląd Spawalnictwa, 2017, no. 5, pp. 109-116.
- [5] Wyględacz B., Kik T., Janicki D.: *Symulacja numeryczna i badania cykli cieplnych hartowania laserowego stali narzędziowej WCL*. Przegląd Spawalnictwa, 2017, no. 5, pp. 91-95.
- [6] *MSC.Marc Volume A, Theory and User Information version*, 2005.
- [7] Kokot G., John A., Kuś W.: *The evolutionary optimization of selected welded structures*. Journal of Achievements in Materials and Manufacturing Engineering, 2010, no. 43, pp. 667-675.
- [8] Gery D., Long H., Maropoulos P.: *Effects of welding speed, energy input and heat source distribution on temperature variations in butt joint welding*. Journal of Materials Processing Tech., 2005, no. 167, pp. 393-401.
<http://dx.doi.org/10.1016/j.jmatprotec.2005.06.018>
- [9] Zhang W., Elmer J.W., DebRoy T.: *Modeling and real time mapping of phases during GTA welding of 1005 steel*. Materials Science and Engineering, 2002, no. A333, pp. 320-335.
[http://dx.doi.org/10.1016/S0921-5093\(01\)01857-3](http://dx.doi.org/10.1016/S0921-5093(01)01857-3)
- [10] Kik T., Slováček M., Wyględacz B.: *Analiza numeryczna procesu spawania wielościgowego złącza teowego oraz obróbki cieplnej po spawaniu*. Przegląd Spawalnictwa, 2016, no. 5, pp. 101-106.
- [11] Kik T.: *Numerical analysis of MIG welding of butt joints in aluminium alloy*. Biuletyn Instytutu Spawalnictwa w Gliwicach, 2014, no. 3, pp. 37-45
<http://bulletin.is.gliwice.pl/article/numerical-analysis-mig-welding-butt-joints-aluminium-alloy>
- [12] Smolik G.: *Private communication*. Idaho National Engineering Laboratories, Idaho Falls, Idaho, 1984.
- [13] Fassani R.N.S., Trevisan O.V.: *Analytical Modeling of Multipass Welding Process with Distributed Heat Source*. Journal of the Brazilian Society of Mechanical Sciences and Engineering, 2003, no. 25, pp. 302-305.
<http://dx.doi.org/10.1590/S1678-58782003000300013>
- [14] Iacobescu G.: *A theoretical model for welding process with Gaussian heat source*. U.P.B. Sci. Bull., 2006, no. 68, pp. 45-50.
- [15] Rouquette S. et al.: *Estimation of the parameters of a Gaussian heat source by the Levenberg–Marquardt method: Application to the electron beam welding*. International Journal of Thermal Sciences, 2007, no. 46, pp. 128-138.
<http://dx.doi.org/10.1016/j.ijthermalsci.2006.04.015>
- [16] Li T.Q., Wu C.S., Feng Y.H., Zheng L.C.: *Modeling of thermal fluid flow and keyhole in stationary plasma arc welding*. International Journal of Heat and Fluid Flow, 2012, no. 34, pp. 117-125.
<http://dx.doi.org/10.1016/j.ijheatfluidflow.2011.12.004>
- [17] Xiang Z. J., Li J. L.: *A conduction model for deep penetration laser welding based on actual keyhole*. Optics & Laser Technology, 2003, no. 35, pp. 5-12.
[http://dx.doi.org/10.1016/S0030-3992\(02\)00116-0](http://dx.doi.org/10.1016/S0030-3992(02)00116-0)
- [18] Giętka T., Ciechacki K., Kik T.: *Numerical Simulation of Duplex Steel Multipass Welding*. Archives of Metallurgy and Materials, 2016, no. 4, pp. 1975-1984.
<http://dx.doi.org/10.1515/amm-2016-0319>